Danthron, an Anthraquinone Derivative, Induces DNA Damage and Caspase Cascades-Mediated Apoptosis in SNU-1 Human Gastric Cancer Cells through Mitochondrial Permeability Transition Pores and Bax-Triggered Pathways

Jo-Hua Chiang,[†] Jai-Sing Yang,[‡] Chia-Yu Ma,[§] Mei-Due Yang,[#] Hui-Ying Huang,[⊥]
Te-Chun Hsia,[▲,⊗] Hsiu-Maan Kuo,[♦] Ping-Ping Wu,[▼] Tsung-Han Lee,[†] and
Jing-Gung Chung*[,△,●]

*Department of Life Sciences, National Chung Hsing University, Taichung 402, Taiwan Department of
Pharmacology, China Medical University, Taichung 404, Taiwan Department of Food and Beverage
Management, Technology and Science Institute of Northern Taiwan, Taipei 112, Taiwan Department of Surgery,
China Medical University Hospital, Taichung 404, Taiwan Department of Nutrition, China Medical University,
Taichung 404, Taiwan School of Chinese Medicine, China Medical University, Taichung 404, Taiwan
Department of Internal Medicine, China Medical University Hospital, Taichung 404, Taiwan Department of
Parasitology, China Medical University, Taichung 404, Taiwan School of Pharmacy, China Medical University,
Taichung 404, Taiwan Department of Biological Science and Technology, China Medical University, No. 91
Hsueh-Shih Road, Taichung 404, Taiwan Department of Biotechnology, Asia University, Taichung 413, Taiwan*

Anthraquinones have been shown to induce apoptosis in different types of tumor cells, but the mechanisms of danthron-induced cytotoxicity and apoptosis in human gastric cancer cells have not been adequately explored. This study investigated the roles of caspase cascades, ROS, DNA damage, mitochondrial disruption, and Bax and Bcl-2 proteins in danthron-induced apoptosis of SNU-1 human gastric cancer cells, a commonly used cell culture system for in vitro studies. Cells were incubated with different concentrations of danthron in a time- and/or dose-dependent manner. Cell morphological changes (shrinkage and rounding) were examined by a phase-contrast microscope, whereas cell viability and apoptotic populations were determined by flow cytometric analysis using propidium iodide (PI) and annexin V−FITC staining. The fluorescent DAPI nucleic acid stain and Comet assay were applied to detect danthron-induced chromatin condensation (an apoptotic characteristic) and DNA damage. Increasing the levels of caspase-3, -8, and -9 activities was involved in danthron-induced apoptosis, and they could be attenuated by inhibitors of specific caspases, indicating that danthron triggered the caspase-dependent apoptotic pathway. Further studies with flow cytometric analyses indicated that cellular levels of ROS, cytosolic Ca^{2+}, and mitochondrial permeability transition (MPT) pore opening were increased, but the level of mitochondrial membrane potential ($\Delta\Psi_m$) was decreased. Also, the ratio of Bax/Bcl-2 levels and other proapoptotic proteins associated with modulating the $\Delta\Psi_m$ were up-regulated. Apoptotic signaling was also stimulated after exposure to danthron and determined by Western blotting and real-time PCR analyses. In summary, it is suggested that danthron-induced apoptotic cell death was involved in mitochondrial depolarization, which led to release of cytochrome *c*, apoptosis-inducing factor (AIF), and endonuclease G (Endo G) and caused the activation of caspase-9 and -3 in SNU-1 human gastric cancer cells.

Introduction

Gastric cancer continues to be a major health problem worldwide (*1, 2*), and current systemic therapies for gastric cancer are often limited by their short-term efficacy due to the side effects (*3, 4*). There are growing interests in the treatment of cancers by using naturally occurring compounds with chemopreventive and chemotherapeutic properties (*5−7*). It is well-known that anticancer properties of these natural herbal compounds can be mediated through different mechanisms. These mechanisms include carcinogen metabolism, induction of DNA damage, immune responses, suppression of cell cycle progression, and/or induction of apoptosis (*8−10*). The best strategy for killing cancer cells is through the induction of apoptosis. It has been widely reported that cancer cell death/apoptosis could be considered a convergence point of all antineoplastic therapies, and bioactive phytochemicals have direct proapoptotic effects (*11, 12*).

Danthron (1,8-dihydroxyanthraquinone), a naturally occurring component, was isolated from the root and rhizome of *Rheum*

* Author to whom correspondence should be addressed (phone +886-4-2205-3366, ext 2161; fax +886-4-2205-3764; e-mail jgchung@mail.cmu.edu.tw).
† National Chung Hsing University.
‡ Department of Pharmacology, China Medical University.
§ Technology and Science Institute of Northern Taiwan.
# Department of Surgery, China Medical University Hospital.
⊥ Department of Nutrition, China Medical University.
▲ School of Chinese Medicine, China Medical University.
⊗ Department of Internal Medicine, China Medical University Hospital.
♦ Department of Parasitology, China Medical University.
▼ School of Pharmacy, China Medical University.
△ Department of Biological Science and Technology, China Medical University.
● Asia University.

palmatum L. (Polygonaceae; Chinese name, Da Huang), a plant used medicinally for a long time (*13–16*). Danthron treatment may, in part, reduce neurotoxicity related to β-amyloid protein (*17*). It was also reported that after daily oral administration of danthron to melanosis coli in the guinea pig large intestine, there was a transient and dose-related wave of apoptosis of the colonic surface epithelial cells (*18*). Moreover, danthron induced the genotoxic potency in L5178Y mouse lymphoma cells (*19*) and intestinal tumors in rats (*20*). Danthron also inhibited human immunodeficiency virus type 1 (HIV-1) integrase (*21*) and suppressed metastatic activity in B16-F10 murine melanoma cells (*22*). Our previous studies have shown that danthron could induce apoptosis and inhibit the migration and invasion in GBM 8401 human brain glioblastoma multiforms cells (*23, 24*). However, there is no study addressing danthron-induced apoptosis in human gastric cancer cells.

The aim of this study was to examine the hypothesis that danthron affected the cytotoxic and apoptotic responses on SNU-1 human gastric cancer cells in vitro. Herein, we also explored the roles of caspase cascades, ROS, DNA damage, mitochondrial dysfunction, and the level of Bax/Bcl-2 ratio in danthron-induced apoptosis of SNU-1 human stomach cancer cells.

Experimental Procedures

Chemicals and Reagents. Danthron, DMSO,[1] PI, NAC, and Triton X-100 were obtained from Sigma-Aldrich Corp. (St. Louis, MO). Fetal bovine serum (FBS), L-glutamine, penicillin–streptomycin, and trypsin–EDTA were obtained from Invitrogen Life Technologies (Carlsbad, CA). The fluorescent probes DAPI, H_2DCF-DA, Indo 1/AM, and $DiOC_6(3)$ and a MitoProbe Transition Pore Assay Kit were purchased from Invitrogen. A Mitochondria/Cytosol Fractionation Kit was obtained from BioVision, Inc. (Mountain View, CA). Caspase substrate reagent kits (PhiPhiLux-G_1D_2, CaspaLux8-L_1D_2, and CaspaLux9-M_1D_2) were bought from OncoImmunin, Inc. (Gaithersburg, MD). The inhibitors of caspases were purchased from R&D Systems (Minneapolis, MN). All primary and secondary antibodies were obtained from Santa Cruz Biotechnology, Inc. (Santa Cruz, CA).

Cell Culture. The SNU-1 human gastric cancer cell line was obtained from the Food Industry Research and Development Institute (Hsinchu, Taiwan). Cells were cultured in RPMI 1640 medium (Invitrogen) supplemented with 10% FBS, 2 mM L-glutamine, 100 units/mL penicillin, and 100 μg/mL streptomycin under a humidified 5% CO_2/95% air atmosphere and grown at 37 °C and 1 atm in an incubator (*25*).

Determinations of Cell Morphology, Cell Viability, and Apoptosis. Cells (2×10^5 cells/well) grown in 12-well plates were treated with DMSO alone (0.1% in medium served as a vehicle control) and different concentrations of danthron (25, 50, 75, 100, and 150 μM). After danthron treatment for 24, 48, and 72 h, cells were photographed under a phase-contrast microscope before being harvested. For viability determination by the PI exclusion method, cells were stained with PI (5 μg/mL) and analyzed with a flow cytometer (Becton Dickinson FACSCalibur, Franklin Lakes, NJ) equipped with an argon ion laser at 488 nm wavelength as previously described (*26*). Cells (1×10^5 cells/mL) were incubated in the presence of 75 μM danthron for 3, 6, and 12 h, and apoptotic cells were stained with annexin V following the manufacturer's

protocol (Annexin V–FITC Apoptosis Detection Kit, BD Pharmingen, San Diego, CA). Subsequently, cells were analyzed by flow cytometry and BD CellQuest Pro software under the examination of FL1 channel for FITC and FL2 detector for PI as described elsewhere (*27, 28*).

Assessments of DAPI Staining, Comet Assay, and DNA Gel Electrophoresis. Cells (1×10^5 cells/mL) in 12-well plates were exposed to 0, 25, 50, 75, 100, and 150 μM danthron for 48 h. Cells were then stained with DAPI (10 μg/mL) after fixation in 4% formaldehyde (Sigma-Aldrich Corp.) and photographed using a fluorescence microscope as previously described (*29, 30*). For Comet assay, cells were harvested and then DNA damage was determined as described elsewhere (*27, 31*). Comet tails were acquired by using CometScore software (Tritek Corp, Sumerduck, VA). Comet tail length was calculated, quantified, and expressed (fold of control) in mean $\pm$ SD ($n = 3$). Approximately 1×10^6 cells per dish were incubated with 75 μM danthron for different intervals of time. Cells were harvested from each sample, and the DNA was isolated for DNA agarose gel electrophoresis. After ethidium bromide (Invitrogen) was used for staining the DNA, the gel was photographed under UV light as previously described (*32*).

Assays of ROS Production, Cytosolic Ca^{2+} Levels, $\Delta\Psi_m$, and MPT Pores. Cells (1×10^5 cells/mL) were seeded in 12-well plates and treated with 75 μM danthron for 1, 3, 6, 12, 24, 48, or 72 h. Cells were harvested, washed twice, and resuspended in the ROS indicator H_2DCF-DA (10 μM), Ca^{2+} probe Indo 1/AM (3 μg/mL), and the $\Delta\Psi_m$ fluorochrome $DiOC_6(3)$ (1 μmol/L) at 37 °C for 30 min. Flow cytometric analyses were used to detect the influences on the levels of ROS, cytosolic Ca^{2+}, and $\Delta\Psi_m$, respectively, as described elsewhere (*31*). The MitoProbe Transition Pore Assay Kit (Invitrogen) was applied to study the opening of MPT pores in danthron-treated SNU-1 cells. When calcein/AM entered the cytoplasm after esterase hydrolysis, calcein distribution was observed in mitochondria and cytosol, and then cobalt chloride ($CoCl_2$) was added to quench cytosolic fluorescence calcein. The procedures were performed according to the instructions provided by the manufacturer (*32, 33*).

Detection of Caspase-3, -8, and -9 Activity and Specific Caspase Inhibitors Pretreatment. Approximately 2×10^5 cells/mL were pretreated with or without the caspase-3 inhibitor (Z-DEVD-FMK), caspase-8 inhibitor (Z-IETD-FMK), caspase-9 inhibitor (Z-LEHD-FMK), and a general caspase inhibitor (Z-VAD-FMK) for 3 h before cells were exposed to 75 μM danthron for 24 h. Cells were harvested for determining the caspase-3, -8, and -9 activities according to the manufacturer's guidelines (PhiPhiLux G_1D_2, CaspaLux 8-L_1D_2, and CaspaLux 9-M_1D_2 kits) (*31*) and the viability of danthron-treated SNU-1 cells as described elsewhere (*27*).

Protein Expression and Subcellular Fractions for Western Blotting Analysis. Approximately 5×10^6 cells were treated with 75 μM danthron for 0, 6, 12, 24, 48, and 72 h. The total proteins from each treatment group were collected, and the levels of apoptosis-modulating proteins were determined as described elsewhere (*32*). The levels of apoptotic proteins are associated with mitochondrial regulations, a hallmark of endoplasmic reticulum (ER) stress and caspase cascades. Equal amounts of protein (40 μg) from each sample were separated by 10–12% sodium dodecyl sulfate–polyacrylamide gel electrophoresis (SDS-PAGE) and transferred to polyvinylidene difluoride membranes by using an iBot Dry Blotting System (Invitrogen). The level of cytochrome *c* in the mitochondria and cytosol was isolated according to the manufacturer's protocol (Mitochondria/Cytosol Fractionation Kit). Cells after treatment with 75 μM danthron were harvested, disrupted, and then centrifuged to isolate cytosolic and mitochondrial fractions, which underwent further examinations by Western blotting analysis as previously described (*29, 32*). The relative abundance of each band was quantified by using ImageJ software (version 1.43, NIH, USA) for Windows (*34*).

---

[1] Abbreviations: AIF, apoptosis-inducing factor; Bax, Bcl-2-associated X protein; Bcl-2, B-cell lymphoma 2; DAPI, 4,6-diamidino-2-phenylindole dihydrochloride; $\Delta\Psi_m$, mitochondrial membrane potential; $DiOC_6(3)$, 3,3′-dihexyloxacarbocyanine iodide; DMSO, dimethyl sulfoxide; Endo G, endonuclease G; FITC, fluorescein isothiocyanate; GST, glutathione transferases; H_2DCF-DA, 2′,7′-dichlorofluorescin diacetate; MPT, mitochondrial permeability transition; NAC, *N*-acetyl-L-cysteine; PI, propidium iodide; SOD, superoxide dismutases.

Table 1. Primer Sequences for Real-Time PCR[a]

primer name	primer sequence (5'−3')
caspase-3	sense, CAGTGGAGGCCGACTTCTTG antisense, TGGCACAAAGCGACTGGAT
caspase-8	sense, GGATGGCCACTGTGAATAACTG antisense, TCGAGGACATCGCTCTCTCA
caspase-9	sense, TGTCCTACTCTACTTTCCCAGGTTTT antisense, GTGAGCCCACTGCTCAAAGAT
AIF	sense, GGGAGGACTACGGCAAAGGT antisense, CTTCCTTGCTATTGGCATTCG
Endo G	sense, GTACCAGGTCATCGGCAAGAA antisense, CGTAGGTGCGGAGCTCAATT
GAPDH	sense, ACACCCACTCCTCCACCTTT antisense, TAGCCAAATTCGTTGTCATACC

[a] Casapse, cysteine aspartate-specific protease; AIF, apoptosis-inducing factor; Endo G, endonuclease G; GAPDH, glyceraldehydes-3-phosphate dehydrogenase. Each assay was conducted at least in triplicate to ensure reproducibility.

Levels of mRNA Expression and Real-Time PCR. Cells (5×10^6 cells) were incubated with 75 μM danthron for 24 and 48 h before total RNA was extracted by using the Qiagen RNeasy Mini Kit (Qiagen, inc, Valencia, CA) as previously described (35). RNA sample was then reverse-transcribed for 30 min at 42 °C with a High Capacity cDNA Reverse Transcription Kit according to the standard protocol of the supplier (Applied Biosystems, Carlsbad, CA). Quantitative PCR was performed by the following conditions: 2 min at 50 °C, 10 min at 95 °C, and 40 cycles of 15 s at 95 °C, 1 min at 60 °C using 1 μL of the cDNA reverse-transcribed as described above, 2× SYBR Green PCR Master Mix (Applied Biosystems), and 200 nM forward and reverse primers as shown in Table 1. Each assay was run on an Applied Biosystems 7300 Real-Time PCR system in triplicate, and fold changes in expression were derived using the comparative C_T method (27, 35).

Immunofluorescence Staining and Confocal Laser Scanning Microscopy. Cells (5×10^4 cells/well) were plated in 4-well chamber slides and incubated with 75 μM danthron for 24 h. Then cells were fixed in 4% formaldehyde for 15 min and permeabilized with 0.1% Triton-X 100 for 30 min with blocking of nonspecific binding sites using 2% bovine serum albumin (BSA) as described elsewhere (31). Fixed cells were incubated with the primary antibodies to cytochrome c, AIF, and Endo G (1:100 dilution) overnight and then exposed to the secondary antibody (FITC-conjugated goat anti-mouse IgG at 1:100 dilution) (green fluorescence) at 37 °C for 2 h. Mitochondria and nuclei were counterstained individually with MitoTracker Red CMXRos (Invitrogen) and PI, respectively (red fluorescence). Photomicrographs were obtained using a Leica TCS SP2 confocal spectral microscope (31).

Statistical Analysis. All data were expressed as the mean ± standard deviation (SD) and performed in triplicate. Statistical analyses were performed using the statistical software SPSS 14.0
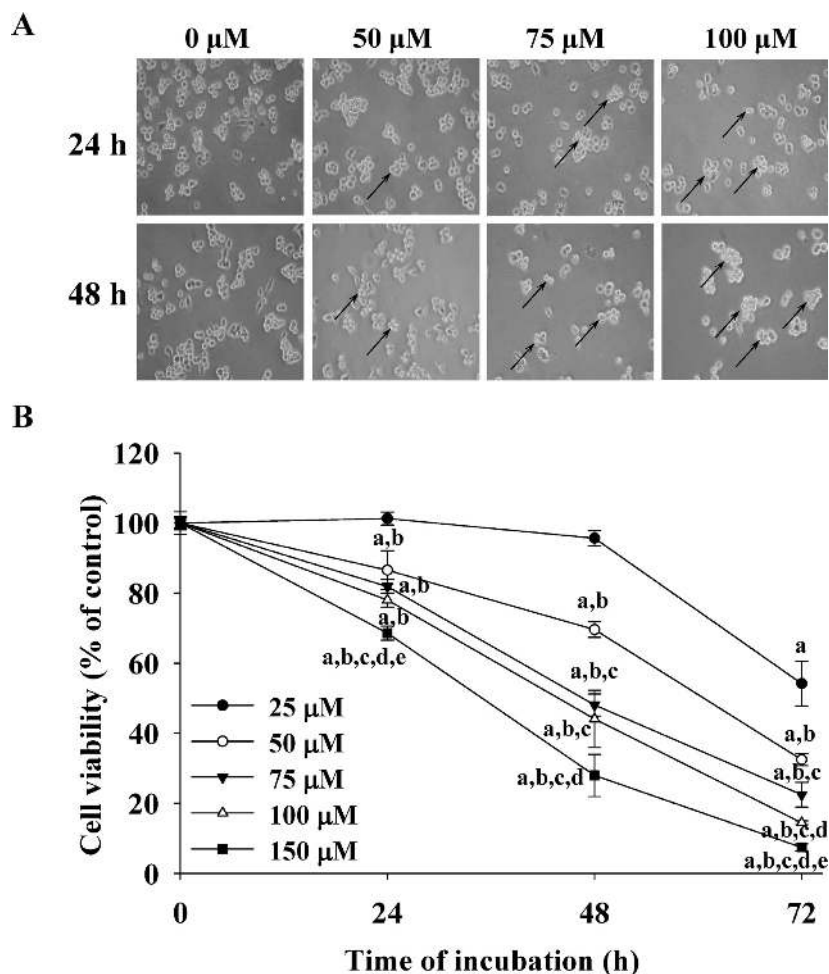

Figure 1. Danthron induced morphological changes and decreased the viability in SNU-1 human gastric cancer cells. Cells were treated with various concentrations of danthron and then were investigated for the cells' morphological changes such as shrinkage and rounding (A), which were photographed at a magnification of 100×. The symbol ↑ reveals the shrinkage and rounding of apoptotic cells. The percentage of viable cells (B) was determined by flow cytometric analysis as described under Experimental Procedures. Data are presented as mean ± SD ($n = 3$). a, $p < 0.05$, is significantly different compared with the DMSO-treated control; b, c, d, and e, $p < 0.05$, are significantly different with 25, 50, 75, and 100 μM danthron treatment, respectively, by one-way ANOVA followed by Bonferroni's test for multiple comparisons.
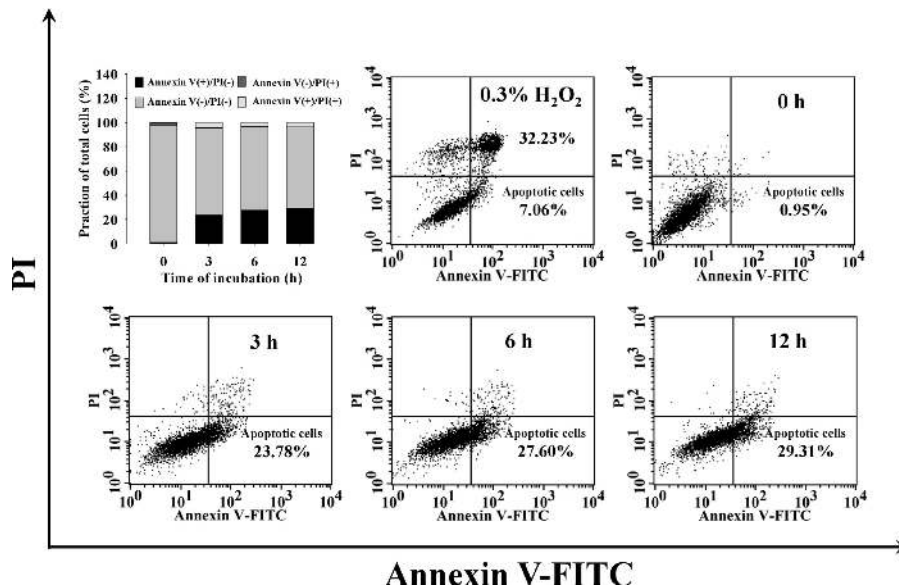
Figure 2. Danthron induced apoptotic cell death in SNU-1 cells. Cells were exposed to 75 μM danthron for 3, 6, and 12 h and then were investigated for the percentage of apoptotic cells as described under Experimental Procedures. The representative profile from flow cytometric analysis is shown, and apoptotic cells were evaluated by annexin V/PI staining. The effect of 0.3% hydrogen peroxide (H_2O_2) treatment is that it is a positive control group. Values shown are representative experiment in triplicate with similar results.
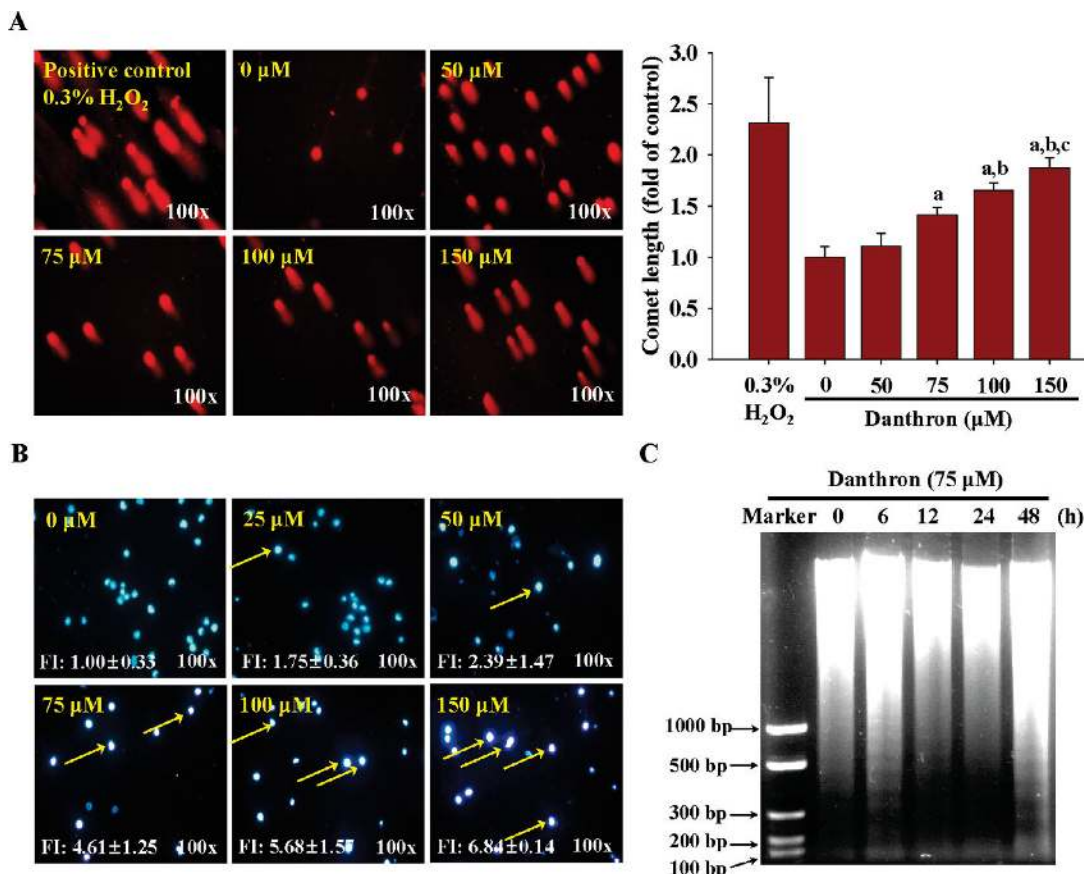

Figure 3. Danthron caused DNA damage and apoptosis. Cells were grown in the presence of different concentrations of danthron for 48 h, and then DNA was isolated from examined cells for Comet assay (A), DAPI staining (B), and DNA gel electrophoresis (C) as described under Experimental Procedures. The arrow (↑) shows chromatin condensation and higher fluorescence intensity in apoptotic cells when compared to the control group. The images were observed and captured using a fluorescent microscope (100×). FI indicates the fluorescence intensity (fold of control), and each value is the mean $\pm$ SD of three experiments. a, $p < 0.05$, is significantly different compared with control; b and c, $p < 0.05$, reveal significant difference compared with 75 and 100 μM danthron treatment, respectively (one-way ANOVA followed by Bonferroni's test for multiple comparisons).

(SPSS Inc., Chicago, IL). One-way ANOVA was used to examine the significance of differences in measured variables between control and treated groups followed by Bonferroni's multiple-comparison test or Student's t test. Differences among groups were considered to be statistically significant when p was <0.05.

Results

Cytotoxicity and Reduction of Viability in SNU-1 Cells after Danthron Treatment. The potential cytotoxic effects of danthron on SNU-1 cells were investigated for morphological
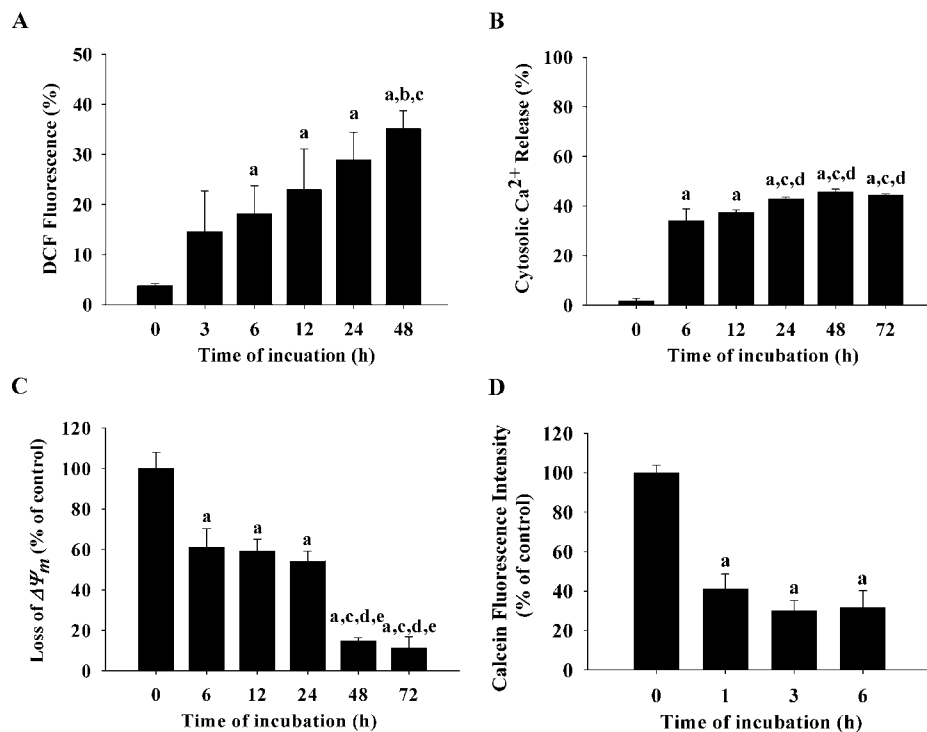
A

B

C

D

Figure 4. Danthron promoted ROS production, cytosolic Ca^{2+} release, loss of $\Delta\Psi_m$, and MPT pore opening in SNU-1 cells. Cells were incubated with 75 μM danthron for various periods of time and then were harvested for examining the ROS generation (A) and cytosolic Ca^{2+} release (B) and for determining the levels of $\Delta\Psi_m$ (C) and MPT pore (D) as described under Experimental Procedures. The results are shown as mean $\pm$ SD ($n = 3$). a, $p < 0.05$, is significantly different compared to control; b, c, d, and e represent significant difference ($p < 0.05$) compared with 75 μM danthron treatment for 3, 6, 12, and 24 h, respectively, by one-way ANOVA followed by Bonferroni's test for multiple comparisons.

changes and cell viability by the phase-contrast microscope and PI exclusion method. Figure 1A shows that SNU-1 cells treated with danthron were subjected to dose-dependent morphological changes such as shrinkage and rounding. Danthron decreased the percentage of viable cells (Figure 1B), and the approximate IC$_{50}$ value was 75 μM after 48 h of treatment. Therefore, we investigated whether danthron could be related to apoptotic cell death. The results from flow cytometric assay reveal that danthron-induced apoptotic cells (annexin V−FITC positive and PI negative) increased when compared to the control group (Figure 2). However, danthron had no significant effect on cell viability in normal cell lines (Supporting Information Figure S1). Normal cell lines included rat embryo aortic smooth muscle cell line (A10), normal fetal osteoblast cell line (hFOB), and normal hepatocyte cell line (Chang liver).

Danthron Induced DNA Damage and Chromatin Condensation. To investigate danthron-induced apoptotic cell death through DNA damage, cells were treated with danthron before analyses with Comet assay, DAPI staining, and DNA gel electrophoresis. Figure 3 reveals that danthron induced SNU-1 cells to undergo dose-dependent DNA damage (Figure 3A), chromatin condensation (an apoptotic characteristic) (Figure 3B), and DNA fragmentation (Figure 3C).

Danthron Promoted ROS Production, Cytosolic Ca^{2+} Release, Loss of $\Delta\Psi_m$, and MPT Pore Opening. The aim was to determine whether danthron-induced DNA damage and apoptosis are involved in these crucial factors in SNU-1 cells. Figure 4 shows that danthron promoted the amount of ROS (Figure 4A), cytosolic Ca^{2+} production (Figure 4B), and opening of the MPT pore (Figure 4D), but depolarized the level of $\Delta\Psi_m$ (Figure 4C) in SNU-1 cells.

Danthron Attenuated Percentage of Viable Cells via Caspase Cascades-Dependent Pathways. Table 2 indicates that danthron-induced apoptosis was mediated by stimulating caspase-

Table 2. Determinations of Caspase-3, -8, and -9 Activity[a]

danthron (75 μM) time of incubation (h)	% of total cells		
	caspase-3	caspase-8	caspase-9
0	1.44 $\pm$ 6.12	3.04 $\pm$ 1.94	3.69 $\pm$ 5.41
6			5.56 $\pm$ 5.88
12		17.98 $\pm$ 3.91*	14.21 $\pm$ 2.96*
24	32.76 $\pm$ 1.38*	36.92 $\pm$ 2.34*	20.89 $\pm$ 4.01*
48	49.56 $\pm$ 0.98*	44.56 $\pm$ 1.34*	17.89 $\pm$ 1.68*
72	48.64 $\pm$ 0.51*	49.29 $\pm$ 0.50*	23.78 $\pm$ 3.71*

[a] Danthron induced the activations of caspases-3, -8, and -9 in SNU-1 cells. The zero hour was defined as untreated control. Cells were treated with 75 μM danthron for indicated periods of time and then harvested for examining the caspase-3, -8, and -9 activity as described under Experimental Procedures. The values are means $\pm$ SD ($n = 3$). *, $p < 0.05$, using one-way ANOVA test followed by Student's t test as compared with 0 h treatment in the presence of danthron exposure.

3, -8, and -9 activities. To investigate if danthron induced apoptosis through the caspase cascades-dependent pathway, cells were individually pretreated with inhibitors of caspase-3, -8, and -9 and a general caspase inhibitor before 75 μM danthron treatment for 24 h. Figure 5 shows that these specific inhibitors significantly suppressed the caspase activities (Figure 5A) and increased the cell viability (Figure 5B) in danthron-treated SNU-1 cells. Cells were also pretreated with Z-VAD-FMK (a general caspase inhibitor) to protect against danthron-induced apoptotic cell death (Figure 5C). These results suggest that the activation of caspases-3, -8, and -9 might be involved in danthron-induced apoptosis in SNU-1 cells.

Danthron Altered Abundance of Apoptosis-Associated Protein and mRNA Expression. To further evaluate the possible signaling pathways for danthron-induced apoptosis, cells were treated with 75 μM danthron for various periods of time. Figure 6 indicates that danthron increased the protein levels of Bcl-$_{XS}$, Bax, and Bid (Figure 6A), cytochrome c, Smac/Diablo, cIAP-2, AIF, and Endo G (Figure 6B), Fas/CD95, Fas
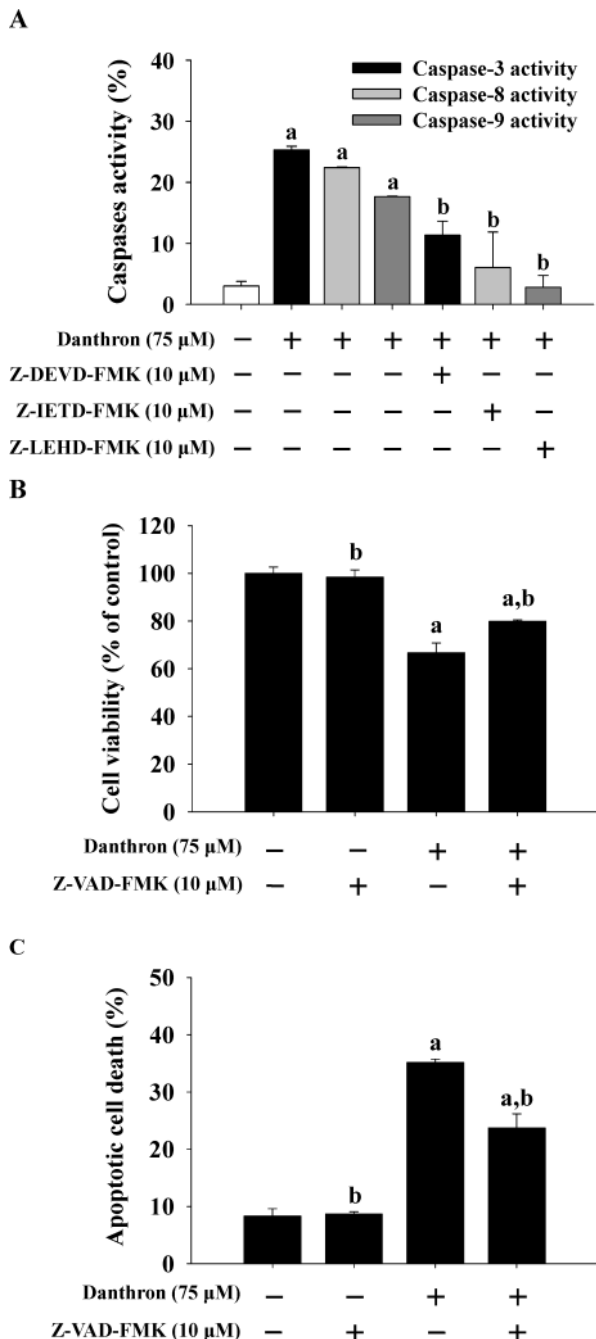
A

B

C

Figure 5. Danthron reduced the percentage of viable cells via a caspase cascade-dependent signaling pathway. SNU-1 cells were pretreated in the presence or absence of the specific inhibitors of caspases-3, -8, -9 and a general caspase inhibitor for 3 h and then were treated with 75 μM danthron for 24 h. Cells were harvested for determining the activities of caspases-3, -8, -9 (A), the percentage of viable cells (B), and apoptotic cell death (C) as described under Experimental Procedures. Columns, mean ($n = 3$); bars, SD. a, $p < 0.05$, is significantly different compared with control; b, $p < 0.05$, shows significant difference compared with 75 μM danthron treatment group by one-way ANOVA followed by Bonferroni's multiple-comparison test.

Ligand, TRAIL (Figure 6C), GRP78, GADD153, and ATF-6α (Figure 6D), caspases-9, -8, -3, and -7 (Figure 6E), and GST-3 (Figure 6F), but decreased the protein levels of Bcl-2 and Bcl-XL (Figure 6A), cIAP-1, Survivin, and XIAP (Figure 6B) and SOD (Cu/Zn) and SOD (Mn) (Figure 6F). Figure 6G shows that the level of cytosolic cytochrome *c* was up-regulated in comparison to the cytosolic control sample. We also found that danthron promoted gene expressions of *caspase-3*, *caspase-8*, and *caspase-9*, *AIF*, and *Endo G* (Figure 6H) in SNU-1 cells.

On the basis of these results, we suggest that danthron-induced apoptosis is mediated through induction of the death receptor, mitochondria, and caspase-3, -8, and -9 multiple signaling pathways.

Danthron Stimulated Translocations of Apoptotic Relative Proteins from Mitochondria. Cells were treated or not with 75 μM danthron for 24 h before being stained by the antibodies of cytychrome *c*, AIF, and Endo G, respectively. The results in Figure 7 from confocal microscopy indicate the expressions of cytochrome *c*, AIF, and Endo G in danthron-treated SNU-1 cells. Danthron enhanced cytochrome *c* release from the mitochondria to the cytosol (Figure 7A) and stimulated mitochondria release of AIF (Figure 7B) and Endo G (Figure 7C) to the nuclei when compared to the control sample.

Discussion

Natural products have long been used to prevent and treat diseases, including cancer (*36, 37*). Danthron is one of the components of *R. palmatum* L. (Polygonaceae), which has been used historically as a traditional Chinese herbal medicine. Mori et al. suggest that danthron has carcinogenicity and may induce liver and intestinal tumors at high-dose (0.2 and 1%) treatment (*20, 38, 39*). In our preliminary study, BALB/c *nu/nu* mice were treated with 1.4 and 4.2 mg/kg of danthron by intraperitoneal (ip) injection and 1.4 and 7 mg/kg oral (po) gavage for 30 days. All animals were evaluated by clinical chemistry and immune modulation analyses such as BUN, creatinine, glucose, albumin, LDH, total protein, sGOT, sGPT, CD3, CD19, CD11b, and Mac-3 to monitor the danthron-related toxicity. Our results, which can be seen in Supporting Information Figure S2 and Tables S1 and S2, indicate that no significant differences were noted when compared to the control (normal mice). Importantly, the nude mice after exposure to danthron were shown to have no adverse effect levels of renal, hepatic, and immune response. We selected doses of 1.4, 4.2, and 7 mg/kg danthron according to the results at IC$_{50}$ value from our in vitro study in SNU-1 cells. Therefore, our results provide important and powerful evidence that a lower concentration (<7 mg/kg) of danthron may not influence the animals.

Danthron, an anthraquinone derivative from rhubarb root (Da Huang), bound noncovalently to DNA and inhibited topoisomerase II activity in L5178Y mouse lymphoma cells (*19*). In our study, we investigated whether danthron exhibited cytotoxic and proapoptotic effects on SNU-1 human gastric cancer cells. This is the first report on danthron-induced apoptosis in SNU-1 cells in which the roles of caspase cascades, ROS production, and mitochondrial dysfunction were explored. The present results were consistent with our previous studies in GBM 8401 cells, indicating that danthron possesses anticancer activities in vitro (*23, 24*). In this study, the mechanism of danthron-induced cell death in SNU-1 cells was investigated by addressing the induction of apoptosis. Apoptotic induction in tumor cells is considered to be very useful in the management, therapy, and prevention of cancer (*5, 40*).

Apoptosis is a gene-regulated phenomenon induced by many chemotherapeutic agents in cancer treatment (*41, 42*) and the characters of apoptosis including chromatin condensation, cell and nuclear shrinkage, membrane blebbing, and oligonucleosomal DNA fragmentation (*43, 44*). In our study, apoptotic cell death was determined according to three different methods: detection of annexin V positive population, expression of DAPI staining, and Bax/Bcl-2 ratio. It is well-documented that DNA fragmentation, after staining with a quantitative DNA-binding
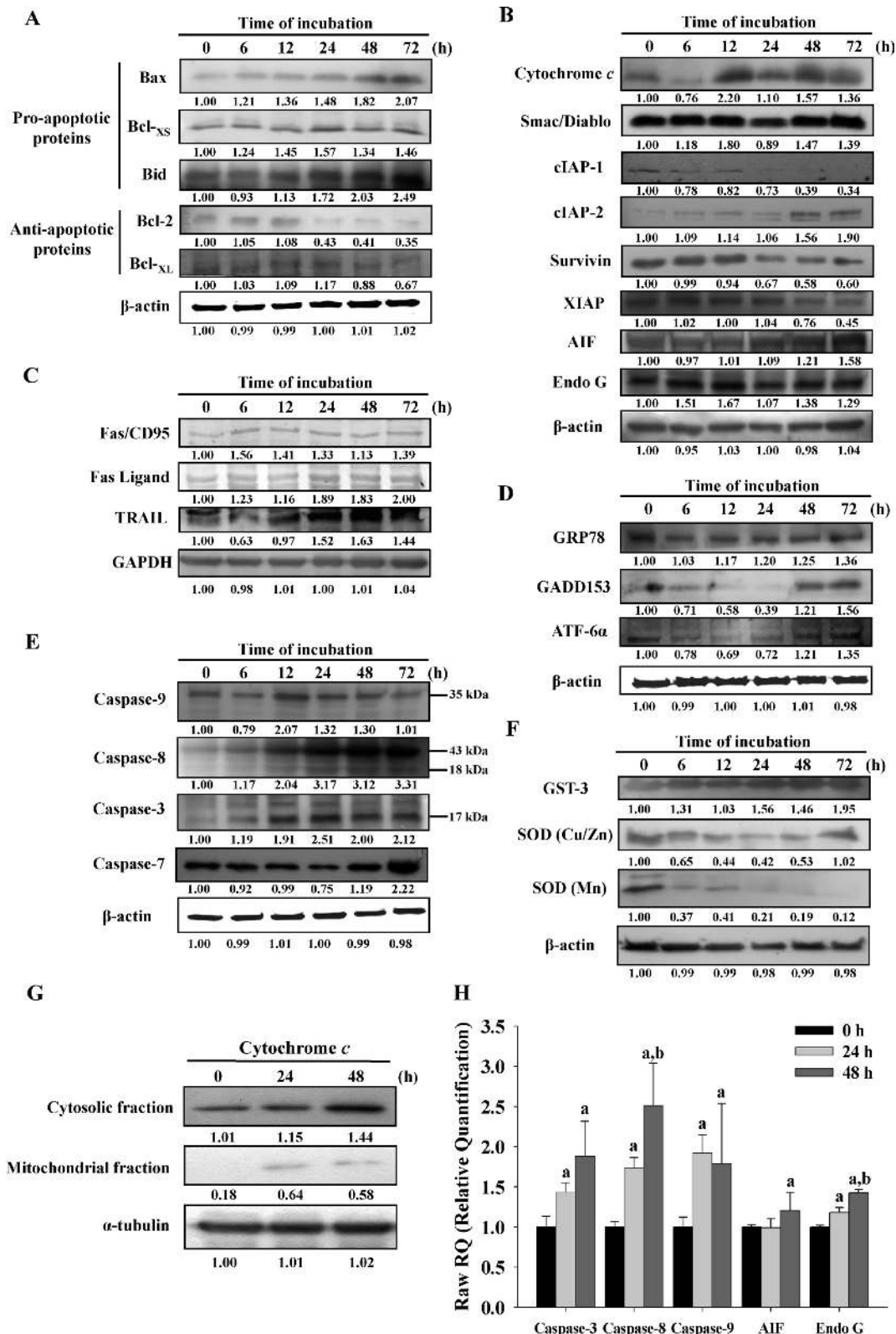
Figure 6. Danthron induced cell death through the effects of apoptosis-related protein and mRNA levels. SNU-1 cells were exposed to 75 μM danthron for various periods of time and harvested for examining the protein levels as shown in panels A–F; the cytochrome c in cytosol and mitochondria fraction were determined (G) as described under Experimental Procedures. The results from real-time PCR analysis for apoptosis-associated mRNA expressions are shown in panel H. Each experiment was done with triple sets: a, $p < 0.05$, shows significant difference compared with 0 h treatment; b, $p < 0.05$, is significantly different compared to danthron treatment for 24 h by one-way ANOVA followed by Bonferroni's multiple-comparison test.

dye such as PI, will cause cells that have lost DNA to take up less stain and appear to the left of the G1 peak in cell cycle distribution by flow cytometric analysis (45). Our results showed that danthron induced a sub-G1 population, which is also

confirmed by annexin V staining. This study indicated that danthron induced apoptotic cell death and promoted G0/G1 phase arrest of cell cycle progression (data not shown) in SNU-1 cells.
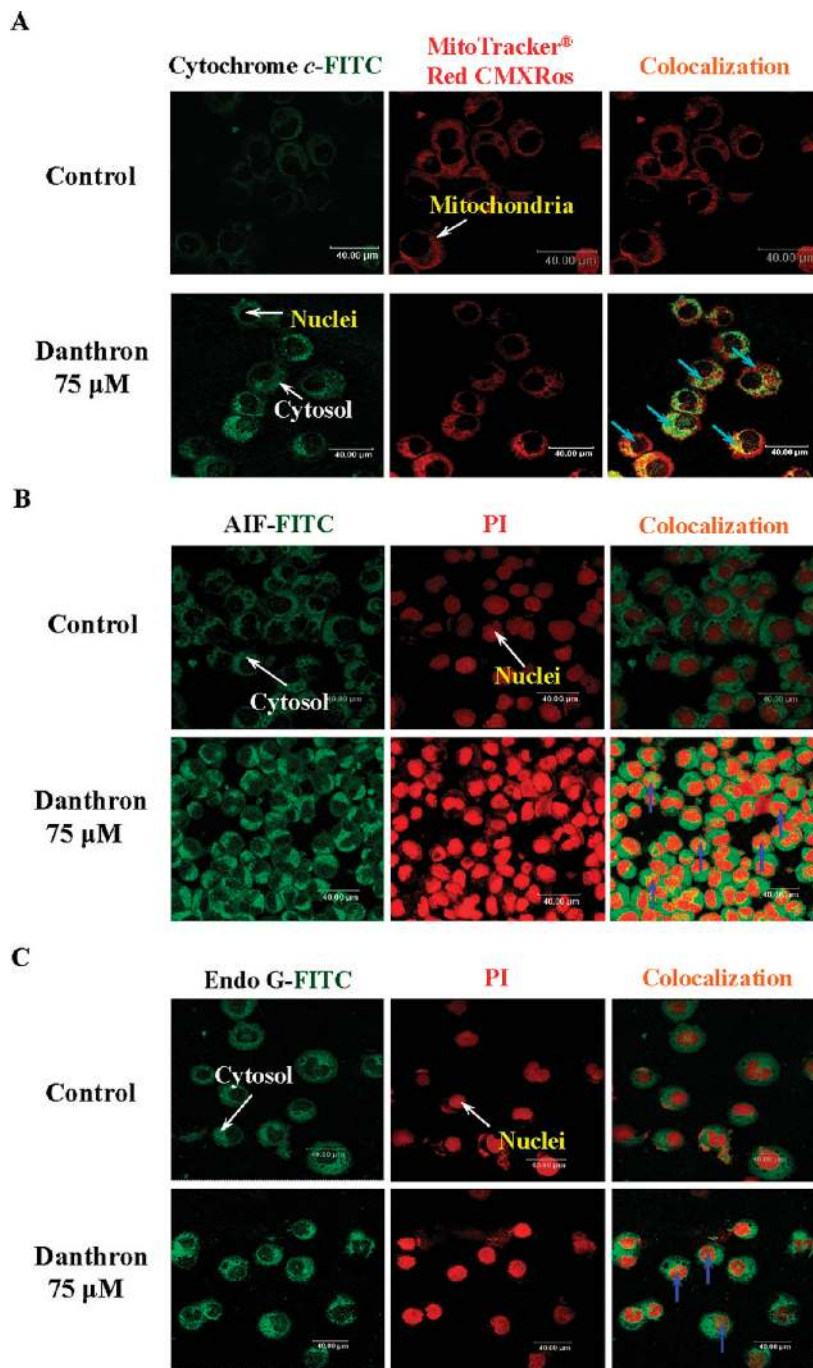
Figure 7. Danthron stimulated the release of apoptosis-associated proteins from mitochondria in SNU-1 cells. Cells (5×10^4 cells/well) plated on 4-well chamber slides were treated without or with 75 μM danthron for 24 h. For observing the distributions of cytochrome *c*, AIF, and Endo G in SNU-1 cells, cells were individually stained with anti-cytochrome *c* (A), anti-AIF (B), and anti-Endo G (C) antibodies, and then FITC-labeled secondary antibodies were used (green fluorescence). Mitochondria and nuclei were counterstained with MitoTracker Red CMXRos and PI, respectively (red color). The images were detected by using a confocal laser scanning microscope as described iunder Experimental Procedures. Scale bar = 40 μm.

It is reported that the activation of caspase cascades appears to be directly responsible for many agents to induce apoptosis in many types of cancer cells (*46*). In this study, reductions of caspase cascades with specific inhibitors could block danthron-induced apoptosis in SNU-1 cells (Figure 5). Results showed that the activations of caspase cascades (Table 2) and some proapoptotic factors (AIF and Endo G) (Figure 7B.C) may be also involved in danthron-treated SNU-1 cells. Cells exposed to danthron led to loss of $\Delta\Psi_m$ and release of cytochrome *c*, AIF, and Endo G. These factors indicated that danthron-induced apoptosis was through mitochondria- and caspase-dependent responses.

The Bcl-2 family, such as pro-apoptotic (Bid, Bax, and Bcl-$_{XS}$) and anti-apoptotic (Bcl-2 and Bcl-$_{XL}$), proteins play important roles in agent-induced apoptosis in cancer cells (*47, 48*). Our results indicated that danthron increased the levels of Bid, Bax, and Bcl-$_{XS}$ (Figure 6A) and decreased the levels of Bcl-2 and Bcl-$_{XL}$ (Figure 6A). The level of Bax expression is an important determining index of apoptotic cell death, which also confirms that the mitochondrial signaling pathway is involved in danthron-induced apoptosis in SNU-1 cells. Once activated, Bax is inserted into the mitochondrial membrane to cause the dysfunction of mitochondria to decrease membrane permeability (*43, 49*), leading to the formation of the MPT pore (*50*). Our

data revealed that danthron depolarized the $\Delta\Psi_m$ (Figure 4C) and stimulated the opening of the MPT pores (Figure 4D) in SNU-1 cells. The MPT pore is accompanied by mitochondrial depolarization, matrix swelling, release of cytochrome c, activation of caspase cascades, and cleavage of downstream death effector proteins and ultimately results in apoptosis (*41, 51*).

In conclusion, the present study offers a novel insight into the cytotoxicity and apoptosis of danthron in a human gastric cancer cell line (SNU-1). ROS affected and promoted a hallmark of several ER stress-related proteins, such as GADD153, GRP78, and ATF-6α. When cytosolic Ca^{2+} was released, Bax/Bcl-2 triggered the apoptotic process through MPT pores. Danthron increased the release of mitochondrial cytochrome c and the activities of caspases-9 and -3. Also, the protein levels of XIAP, cIAP, and survivin were down-regulated and contributed to the activation of caspase-3, leading to cell apoptosis. Additionally, it also stimulated release of AIF and Endo G from mitochondria and trafficking to the nuclei. The addition of danthron treatment is attributed to enhanced levels of Fas/Fas ligand or TRAIL and active caspase-8 signaling. Danthron-induced apoptosis seems to involve DNA damage by affecting ROS production and alterations of SOD or GST. The schematic of the proposed signaling pathways can be seen in the Table of Contents graphic.

Supporting Information Available: Additional experimental methods, references, figures, and tables. This material is available free of charge via the Internet at http://pubs.acs.org.

References

(1) Winawer, S. J. (2005) Gastric cancer: worldwide burden and prevention opportunities. *Chin. J. Dig. Dis. 6*, 107–109.

(2) Williams, L., Somasekar, A., Davies, D. J., Cronin, J., Doak, S. H., Alcolado, R., Williams, J. G., Griffiths, A. P., Baxter, J. N., and Jenkins, G. J. (2009) Aneuploidy involving chromosome 1 may be an early predictive marker of intestinal type gastric cancer. *Mutat. Res. 669*, 104–111.

(3) Palesty, J. A., Wang, W., Javle, M. M., and Yang, G. Y. (2004) Side effects of therapy: case 3. Gastric cancer after radiotherapy of pediatric Hodgkin's disease. *J. Clin. Oncol. 22*, 2507–2509.

(4) Yu, G., Ren, D., Sun, G., and Zhang, D. (1993) Clinical and experimental studies of JPYS in reducing side-effects of chemotherapy in late-stage gastric cancer. *J. Tradit. Chin. Med. 13*, 31–37.

(5) Ram, V. J., and Kumari, S. (2001) Natural products of plant origin as anticancer agents. *Drug News Perspect. 14*, 465–482.

(6) Hubner, R. A., and Houlston, R. S. (2009) Folate and colorectal cancer prevention. *Br. J. Cancer 100*, 233–239.

(7) Shimizu, M., and Weinstein, I. B. (2005) Modulation of signal transduction by tea catechins and related phytochemicals. *Mutat. Res. 591*, 147–160.

(8) Ko, J. K., Leung, W. C., Ho, W. K., and Chiu, P. (2007) Herbal diterpenoids induce growth arrest and apoptosis in colon cancer cells with increased expression of the nonsteroidal anti-inflammatory drug-activated gene. *Eur. J. Pharmacol. 559*, 1–13.

(9) Hou, Z., Lambert, J. D., Chin, K. V., and Yang, C. S. (2004) Effects of tea polyphenols on signal transduction pathways related to cancer chemoprevention. *Mutat. Res. 555*, 3–19.

(10) Sparreboom, A., Cox, M. C., Acharya, M. R., and Figg, W. D. (2004) Herbal remedies in the United States: potential adverse interactions with anticancer agents. *J. Clin. Oncol. 22*, 2489–2503.

(11) Clark, G. B., Thompson, G., Jr., and Roux, S. J. (2001) Signal transduction mechanisms in plants: an overview. *Curr. Sci. 80*, 170–177.

(12) Lin, H. L., Yang, J. S., Yang, J. H., Fan, S. S., Chang, W. C., Li, Y. C., and Chung, J. G. (2006) The role of Ca^{2+} on the DADS-induced apoptosis in mouse-rat hybrid retina ganglion cells (N18). *Neurochem. Res. 31*, 383–393.

(13) Tsai, T. H., and Chen, C. F. (1992) Ultraviolet spectrum identification of emodin in rabbit plasma by HPLC and its pharmacokinetics application. *Asia−Pac. J. Pharmacol. 7*, 53–56.

(14) Liang, J. W., Hsiu, S. L., Huang, H. C., and Lee-Chao, P. D. (1993) HPLC analysis of emodin in serum, herbs and Chinese herbal prescriptions. *J. Food Drug Anal. 1*, 251–257.

(15) Huang, Q., Lu, G., Shen, H. M., Chung, M. C., and Ong, C. N. (2007) Anti-cancer properties of anthraquinones from rhubarb. *Med. Res. Rev. 27*, 609–630.

(16) Tang, T., Yin, L., Yang, J., and Shan, G. (2007) Emodin, an anthraquinone derivative from *Rheum officinale* Baill, enhances cutaneous wound healing in rats. *Eur. J. Pharmacol. 567*, 177–185.

(17) Kwon, Y. S., Koh, J. Y., Song, D. K., Kim, H. C., Kwon, M. S., Choi, Y. S., and Wie, M. B. (2004) Danthron inhibits the neurotoxicity induced by various compounds causing oxidative damages including β-amyloid (25−35) in primary cortical cultures. *Biol. Pharm. Bull. 27*, 723–726.

(18) Walker, N. I., Bennett, R. E., and Axelsen, R. A. (1988) Melanosis coli. A consequence of anthraquinone-induced apoptosis of colonic epithelial cells. *Am. J. Pathol. 131*, 465–476.

(19) Mueller, S. O., Lutz, W. K., and Stopper, H. (1998) Factors affecting the genotoxic potency ranking of natural anthraquinones in mammalian cell culture systems. *Mutat. Res. 414*, 125–129.

(20) Mori, H., Sugie, S., Niwa, K., Takahashi, M., and Kawai, K. (1985) Induction of intestinal tumours in rats by chrysazin. *Br. J. Cancer 52*, 781–783.

(21) Farnet, C. M., Wang, B., Hansen, M., Lipford, J. R., Zalkow, L., Robinson, W. E., Jr., Siegel, J., and Bushman, F. (1998) Human immunodeficiency virus type 1 cDNA integration: new aromatic hydroxylated inhibitors and studies of the inhibition mechanism. *Antimicrob. Agents Chemother. 42*, 2245–2253.

(22) Rossi, S., Tabolacci, C., Lentini, A., Provenzano, B., Carlomosti, F., Frezzotti, S., and Beninati, S. (2010) Anthraquinones danthron and quinizarin exert antiproliferative and antimetastatic activity on murine B16-F10 melanoma cells. *Anticancer Res. 30*, 445–449.

(23) Lu, H. F., Wang, H. L., Chuang, Y. Y., Tang, Y. J., Yang, J. S., Ma, Y. S., Chiang, J. H., Lu, C. C., Yang, J. L., Lai, T. Y., Wu, C. C., and Chung, J. G. (2009) Danthron induced apoptosis through mitochondria- and caspase-3-dependent pathways in human brain glioblastoma multiforms GBM 8401 cells. *Neurochem. Res. 35*, 390–398.

(24) Lin, C. C., Chen, J. T., Yang, J. S., Lu, H. F., Hsu, S. C., Tan, T. W., Lin, Y. T., Ma, Y. S., Ip, S. W., Wu, J. J., Li, Y. C., and Chung, J. G. (2009) Danthron inhibits the migration and invasion of human brain glioblastoma multiforme cells through the inhibition of mRNA expression of focal adhesion kinase, Rho kinases-1 and metalloproteinase-9. *Oncol. Rep. 22*, 1033–1037.

(25) Atten, M. J., Godoy-Romero, E., Attar, B. M., Milson, T., Zopel, M., and Holian, O. (2005) Resveratrol regulates cellular PKC α and δ to inhibit growth and induce apoptosis in gastric cancer cells. *Invest. New Drugs 23*, 111–119.

(26) Yang, P. M., Chen, H. C., Tsai, J. S., and Lin, L. Y. (2007) Cadmium induces Ca^{2+}-dependent necrotic cell death through calpain-triggered mitochondrial depolarization and reactive oxygen species-mediated inhibition of nuclear factor-κB activity. *Chem. Res. Toxicol. 20*, 406–415.

(27) Lu, C. C., Yang, J. S., Huang, A. C., Hsia, T. C., Chou, S. T., Kuo, C. L., Lu, H. F., Lee, T. H., Wood, W. G., and Chung, J. G. (2010) Chrysophanol induces necrosis through the production of ROS and alteration of ATP levels in J5 human liver cancer cells. *Mol. Nutr. Food Res. 54*, 967–976.

(28) Kuo, T. C., Yang, J. S., Lin, M. W., Hsu, S. C., Lin, J. J., Lin, H. J., Hsia, T. C., Liao, C. L., Yang, M. D., Fan, M. J., Wood, W. G., and Chung, J. G. (2009) Emodin has cytotoxic and protective effects in rat C6 glioma cells: roles of Mdr1a and nuclear factor κB in cell survival. *J. Pharmacol. Exp. Ther. 330*, 736–744.

(29) Chung, J. G., Yang, J. S., Huang, L. J., Lee, F. Y., Teng, C. M., Tsai, S. C., Lin, K. L., Wang, S. F., and Kuo, S. C. (2007) Proteomic approach to studying the cytotoxicity of YC-1 on U937 leukemia cells and antileukemia activity in orthotopic model of leukemia mice. *Proteomics 7*, 3305–3317.

(30) Dornetshuber, R., Heffeter, P., Kamyar, M. R., Peterbauer, T., Berger, W., and Lemmens-Gruber, R. (2007) Enniatin exerts p53-dependent cytostatic and p53-independent cytotoxic activities against human cancer cells. *Chem. Res. Toxicol. 20*, 465–473.

(31) Chen, J. C., Lu, K. W., Tsai, M. L., Hsu, S. C., Kuo, C. L., Yang, J. S., Hsia, T. C., Yu, C. S., Chou, S. T., Kao, M. C., Chung, J. G., and Wood, W. G. (2009) Gypenosides induced G0/G1 arrest via CHK2 and apoptosis through endoplasmic reticulum stress and mitochondria-dependent pathways in human tongue cancer SCC-4 cells. *Oral Oncol. 45*, 273–283.

(32) Yang, J. S., Chen, G. W., Hsia, T. C., Ho, H. C., Ho, C. C., Lin, M. W., Lin, S. S., Yeh, R. D., Ip, S. W., Lu, H. F., and Chung, J. G. (2009) Diallyl disulfide induces apoptosis in human colon cancer cell line (COLO 205) through the induction of reactive oxygen species, endoplasmic reticulum stress, caspases casade and mitochondrial-dependent pathways. *Food Chem. Toxicol. 47*, 171–179.

(33) Petronilli, V., Miotto, G., Canton, M., Brini, M., Colonna, R., Bernardi, P., and Di Lisa, F. (1999) Transient and long-lasting openings of the mitochondrial permeability transition pore can be monitored directly in intact cells by changes in mitochondrial calcein fluorescence. *Biophys. J. 76*, 725–734.

(34) Shen, J. K., Du, H. P., Yang, M., Wang, Y. G., and Jin, J. (2009) Casticin induces leukemic cell death through apoptosis and mitotic catastrophe. *Ann. Hematol. 88*, 743–752.

(35) Ji, B. C., Hsu, W. H., Yang, J. S., Hsia, T. C., Lu, C. C., Chiang, J. H., Yang, J. L., Lin, C. H., Lin, J. J., Wu Suen, L. J., Wood, W. G., and Chung, J. G. (2009) Gallic acid induces apoptosis via caspase-3 and mitochondrion-dependent pathways in vitro and suppresses lung xenograft tumor growth in vivo. *J. Agric. Food Chem. 57*, 7596–7604.

(36) Lund, T., Stokke, T., Olsen, O. E., and Fodstad, O. (2005) Garlic arrests MDA-MB-435 cancer cells in mitosis, phosphorylates the proapoptotic BH3-only protein BimEL and induces apoptosis. *Br. J. Cancer 92*, 1773–1781.

(37) Yang, C. S., Wang, X., Lu, G., and Picinich, S. C. (2009) Cancer prevention by tea: animal studies, molecular mechanisms and human relevance. *Nat. Rev. Cancer 9*, 429–439.

(38) Mori, H., Sugie, S., Niwa, K., Yoshimi, N., Tanaka, T., and Hirono, I. (1986) Carcinogenicity of chrysazin in large intestine and liver of mice. *Jpn. J. Cancer Res. 77*, 871–876.

(39) Poginsky, B., Westendorf, J., Blomeke, B., Marquardt, H., Hewer, A., Grover, P. L., and Phillips, D. H. (1991) Evaluation of DNA-binding activity of hydroxyanthraquinones occurring in *Rubia tinctorum* L. *Carcinogenesis 12*, 1265–1271.

(40) Hu, W. P., Yu, H. S., Sung, P. J., Tsai, F. Y., Shen, Y. K., Chang, L. S., and Wang, J. J. (2007) DC-81-Indole conjugate agent induces mitochondria mediated apoptosis in human melanoma A375 cells. *Chem. Res. Toxicol. 20*, 905–912.

(41) Gerl, R., and Vaux, D. L. (2005) Apoptosis in the development and treatment of cancer. *Carcinogenesis 26*, 263–270.

(42) Ward, T. H., Cummings, J., Dean, E., Greystoke, A., Hou, J. M., Backen, A., Ranson, M., and Dive, C. (2008) Biomarkers of apoptosis. *Br. J. Cancer 99*, 841–846.

(43) Green, D. R., and Reed, J. C. (1998) Mitochondria and apoptosis. *Science (New York, N.Y.) 281*, 1309–1312.

(44) Nesslany, F., Simar-Meintieres, S., Ficheux, H., and Marzin, D. (2009) Aloe-emodin-induced DNA fragmentation in the mouse in vivo comet assay. *Mutat. Res. 678*, 13–19.

(45) Yan, B., Wang, H., Li, F., and Li, C. Y. (2006) Regulation of mammalian horizontal gene transfer by apoptotic DNA fragmentation. *Br. J. Cancer 95*, 1696–1700.

(46) Chou, L. C., Yang, J. S., Huang, L. J., Wu, H. C., Lu, C. C., Chiang, J. H., Chen, K. T., Kuo, S. C., and Chung, J. G. (2009) The synthesized 2-(2-fluorophenyl)-6,7-methylenedioxyquinolin-4-one (CHM-1) promoted G2/M arrest through inhibition of CDK1 and induced apoptosis through the mitochondrial-dependent pathway in CT-26 murine colorectal adenocarcinoma cells. *J. Gastroenterol. 44*, 1055–1063.

(47) Gavathiotis, E., Suzuki, M., Davis, M. L., Pitter, K., Bird, G. H., Katz, S. G., Tu, H. C., Kim, H., Cheng, E. H., Tjandra, N., and Walensky, L. D. (2008) BAX activation is initiated at a novel interaction site. *Nature 455*, 1076–1081.

(48) Cai, J., Wang, M., Li, B., Wang, C., Chen, Y., and Zuo, Z. (2009) Apoptotic and necrotic action mechanisms of trimethyltin in human hepatoma G2 (HepG2) cells. *Chem. Res. Toxicol. 22*, 1582–1587.

(49) Green, D. R., and Chipuk, J. E. (2008) Apoptosis: stabbed in the BAX. *Nature 455*, 1047–1049.

(50) Bernardi, P., Krauskopf, A., Basso, E., Petronilli, V., Blachly-Dyson, E., Di Lisa, F., and Forte, M. A. (2006) The mitochondrial permeability transition from in vitro artifact to disease target. *FEBS J. 273*, 2077–2099.

(51) Zhao, M., Zhang, Y., Wang, C., Fu, Z., Liu, W., and Gan, J. (2009) Induction of macrophage apoptosis by an organochlorine insecticide acetofenate. *Chem. Res. Toxicol. 22*, 504–510.